SOAC Exercise 2: The Advection Equation

Peter Farrell, Dong Jian, Jiongqiu Ren

January 6, 2022

1 Introduction

We simulate the linear advection equation using three different numerical schemes, namely the Euler Forward (upwind) method, the Lax-Wendroff scheme, and the spectral method. This series of tests is referred to as the Molenkamp test. Comparing the results after one revolution, we find some schemes exhibit numerical diffusion and that others exhibit numerical dispersion. It is found that the spectral method is the most accurate, since it has very little numerical diffusion and is without numerical dispersion or phase error.

2 Euler Method

In this section, we use the Euler-forward (in time) and upwind (in space) scheme to solve the advection equation numerically. The upwind in space scheme is the least diffusive method we could think of and is more stable than the downwind scheme.

The whole numerical simulation shows an signal moving from the middle of the area to the right boundary, appearing on the left boundary and then ending up in the middle again.

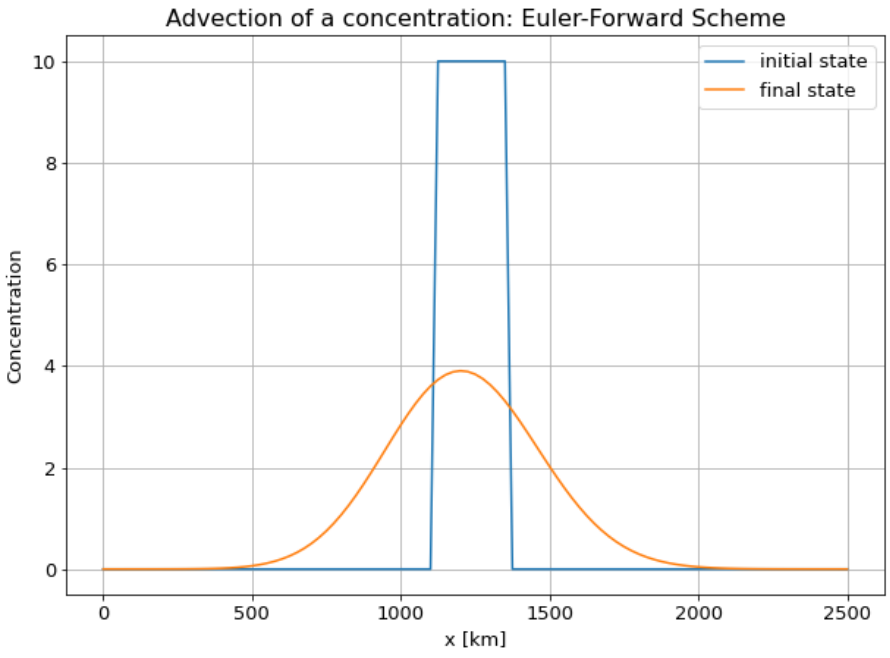

Figure 1: Euler Forward Upwind Scheme

Then we output the results in Figure 1. Figure 1 shows the simulated signal at the initial and final state. According to the figure, we see that the initial numerical signal is pretty well resolved, very close to the analytical one, but the final state of the numerical signal has deformed quite a lot. The amplitude has shrunk and the phase of the peak seems a little bit later − it should have appeared in the middle.

But if we integrate the signal (concentration) over the whole area, we find that the value of the final state is almost the same as the initial state. This can be explained by the truncation error when trying to resolve an incontinuous (abrupt) signal. Specifically, this is a diffusion error.

3 Lax-Wendroff Method

The Lax-Wendroff method is a second order scheme that is accurate in both space and time, and which starts with a Taylor approximation of C_j^{n+1}:

$$C_j^{n+1} = C_j^n + \Delta t \left(\frac{\partial C}{\partial t}\right)_j^n + \frac{\Delta t^2}{2}\left(\frac{\partial^2 C}{\partial t^2}\right)_j^n + \dots \tag{1}$$

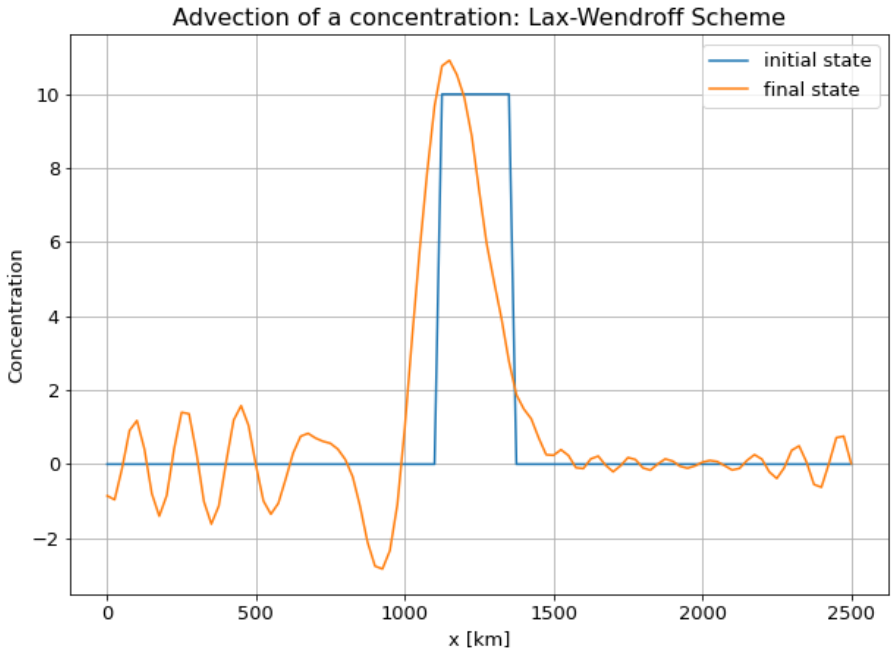

Figure 2: Lax-Wendroff Scheme

From the linear advection equation, we have:

$$\frac{\partial C}{\partial t} = -u_0 \frac{\partial C}{\partial x} \tag{2}$$

$$\frac{\partial^2 C}{\partial t^2} = u_0^2 \frac{\partial^2 C}{\partial x^2} \tag{3}$$

Approximating the spatial derivative by central differences:

$$\left(\frac{\partial C}{\partial x}\right)_j^n \approx \frac{C_{j+1}^n - C_{j-1}^n}{2\Delta x} \tag{4}$$

$$\left(\frac{\partial^2 C}{\partial x^2}\right)_j^n \approx \frac{C_{j+1}^n - 2C_j^n + C_{j-1}^n}{\Delta x^2} \tag{5}$$

By substitution, we get the finite difference approximation to the linear advection equation:

$$\frac{C_j^{n+1} - C_j^n}{\Delta t} \approx -u_0 \left(\frac{C_{j+1}^n - C_{j-1}^n}{2\Delta x}\right) + \frac{u_0^2 \Delta t}{2} \left(\frac{C_{j+1}^n - 2C_j^n + C_{j-1}^n}{\Delta x^2}\right) \tag{6}$$

Constrained by CFL condition, the result for the Lax-Wendroff scheme is shown in Figure 2. In the final state, the concentration in the middle of the domain is close to the initial state, while the maximum concentration exceeds 10 and the lateral domain shows spurious oscillations. This is a truncation error due to numerical dispersion which occurs when a higher order approximation is used to improve accuracy. So we see the so called "spurious oscillations".

4 Spectral Method

In this method, we expand the advection equation as a Fourier series.

$$C(x,t) = Re\{\sum C_k \exp \frac{2\pi i k j}{N}\} \tag{7}$$

As before, we set u_0 and C_0 equal to ten. Additionally, we pick values for dt such that σ is lower than one.

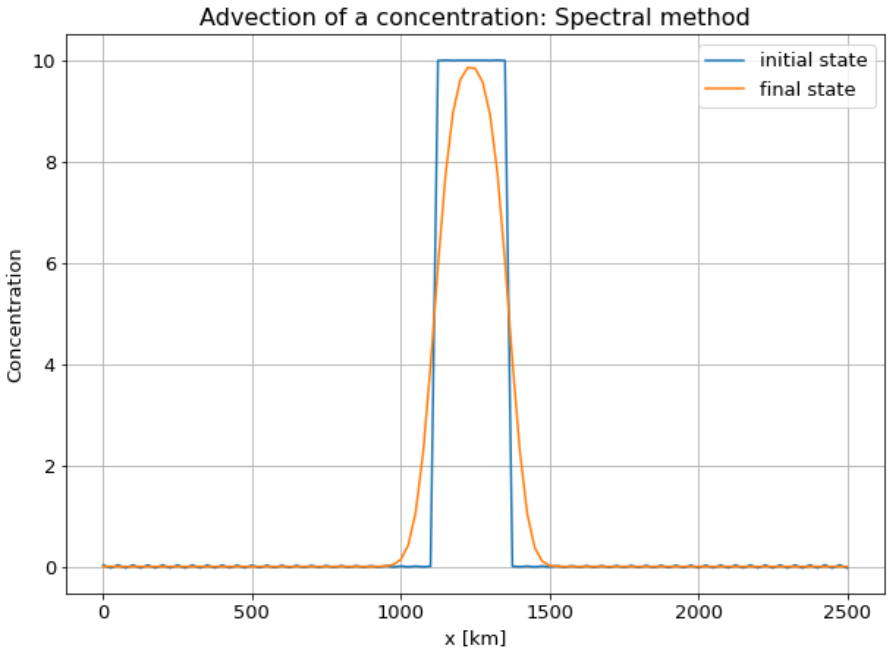

Figure 3: Spectral Method

We then find the Fourier coefficients α and β.

$$\alpha_k = \frac{2}{N} \sum C_j \cos(-2\pi k j / N) \tag{8}$$

$$\beta_k = \frac{2}{N} \sum C_j \sin(-2\pi kj/N) \tag{9}$$

We evaluate these coefficients across all possible values in spectral space and then incorporate in the full Fourier series expression. This is then integrated across all spectral space using the Matsuno time-stepping scheme. This scheme, which comprises predictor and corrector parts, is given below (Equations 10 and 11).

$$\frac{C*_k^{n+1} - C_k^n}{\Delta t} = -\frac{2\pi i u_0 k}{L} C_k^n \tag{10}$$

$$\frac{C_k^{n+1} - C_k^n}{\Delta t} = -\frac{2\pi i u_0 k}{L} C*_k^{n+1} \tag{11}$$

The results are converted from spectral space back into physical space and are plotted in Figure 3. It is clear that the numerical results are in phase with the analytical solution. Also, while there is some diffusion, it is not nearly as significant as it is for the other numerical methods shown previously. It is therefore clear that the spectral scheme is by far the most accurate scheme seen thus far.